38th ERF, September 3–6, 2013, Moscow, Russia

078

Experimental Evaluation of an L-Shaped Tab to be used as an Active Gurney Flap for Dynamic Stall Control

A. Zanotti*, D. Grassi and G. Gibertini

Politecnico di Milano – Dipartimento di Scienze e Tecnologie Aerospaziali
Via La Masa 34, 20156 Milano – Italy
e–mail: *alex.zanotti@polimi.it

Keywords: Aerodynamics, Oscillating Airfoil, Gurney Flap, Dynamic Stall.

Abstract

The present paper describes an experimental activity carried out in the frame of research about dynamic stall control. In particular, an L-shaped tab was tested on the trailing edge of a pitching airfoil in deep dynamic stall condition. The L-shaped tab was tested on a NACA 23012 pitching blade section model in two different fixed positions: deployed and retracted. When deployed the tab is flush to the airfoil upper surface and its end prong behaves as a Gurney flap at the airfoil trailing edge. When retracted the tab features an angle of 9.1 deg. with the airfoil upper surface since its prong tip touches the airfoil trailing edge. The experimental activity includes both unsteady pressure measurements on the airfoil midspan contour to evaluate the airloads time histories and Particle Image Velocimetry (PIV) carried out at the trailing edge region. The experimental results shows that the use of such a pivoting L-shaped tab can introduce similar advantages for dynamic stall alleviation to the ones that can be obtained by the use of an active Gurney flap. Therefore, due to an easier integration on helicopter blades, the tested L-shaped tab can be considered an attractive device to be used on helicopter blades for dynamic stall control.

Nomenclature

c	blade section model chord [m]
C_L	lift coefficient
C_M	pitching moment coefficient about the airfoil quarter chord
C_p	pressure coefficient
DSTA	Dipartimento di Scienze e Tecnologie Aerospaziali
f	oscillation frequency [Hz]
k	reduced frequency, $\equiv \pi f c/U_\infty$
Ma	Mach number
PIV	Particle Image Velocimetry
Re	Reynolds number
$\|U\|$	velocity magnitude [m/s]
U_∞	free-stream velocity [m/s]
x	stream-wise coordinate [m]
α	angle of attack [deg]
α_m	mean angle of attack [deg]
α_a	pitching oscillation amplitude [deg]
ω	circular frequency [rad/s]

1 Introduction

Dynamic stall control has become in the recent years one of the more challenging research topic in rotorcraft aerodynamics field due to the current interest in the design of new active blade concepts developed to overcome the several limitations on helicopter performance introduced by this phenomenon [1, 2, 3]. In fact, many recent activities show the study of different active and passive control devices integrated into a blade section model. In this frame of research, attractive solutions for reducing the airloads hysteresis as well as for the stall-driven flutter suppression [3] rely upon the optimization of the blade airfoil shape through a variable droop leading edge [4] or the use of blowing devices such as air-jet vortex generators [5, 6] or plasma actuators [7].

Another attractive solution to be used in the rotorcraft environment for blade performance improvement is the use of the Gurney flap [8, 9]. In particular, both experimental and numerical activities demonstrated that the lift enhancement mechanism of a Gurney flap [10] can be useful for the alleviation of the dynamic stall detrimental effects on the retreating blade [11]. In fact, the results of numerical simulations report that the use of an active Gurney flap deployed on the retreating side of rotor disk and retracted on the advancing side introduces benefits for rotorcraft performance [12, 13]. These numerical results are also confirmed by the experimental activity carried out on a pitching blade section model equipped with a fixed Gurney flap at the airfoil trailing edge [14, 15].

Nevertheless, the manufacture and the integration of an active Gurney flap on a helicopter blade represents a challenging and costly activity. For instance, one of the most strict requirements is to stow the deployable device, together with the required actuation mechanism, at the blade trailing edge where the limitions in space is very severe. Therefore, the main goal of the present work was to evaluate the performance of a device that behaves as an Gurney flap for dynamic stall alleviation purpose but could be integrated more easily at the trailing edge region of a blade. The present paper describes the experimental investigation of the effects of an L-shaped tab positioned at the trailig edge of on a pitching NACA 23012 blade section model in deep dynamic stall condition [1]. The L-shaped tab was tested in two different fixed positions to evaluate the effects introduced on the aerodynamic performance of the airfoil during a pitching cycle. In particular, lift and pitching moment were evaluated by the integration of pressure measurements carried out on the midspan airfoil contour, while the detailed flow physics concerned with the use of such a device was investigated by PIV surveys at the trailing edge region.

2 Experimental Set up

The experimental activity was carried out using the pitching airfoil rig at Politecnico di Milano (DSTA Aerodynamics Laboratory) [16]. The wind tunnel has a rectangular test section 1.5 m high and 1 m wide. The maximum wind velocity is 55 m/s and the free stream turbulence level is less than 0.1%.

A NACA 23012 airfoil model was used for the current test activity. The NACA 23012 airfoil was object of several experimental activities about the investigation of the fine details of dynamic stall process [17, 18, 19]. The blade section model, has a chord of 0.3 m and a 0.93

m span and it is composed by three aluminium machined section attached to an internal metallic structure. The model has two interchangeable central sections, one equipped with pressure taps positioned along the midspan airfoil contour and another without taps to be used for PIV surveys. The model is pivoted about two external steel shafts with axis at 25% c. End plates were mounted at the model tips during the tests to reduce the interference of the wind tunnel walls boundary layer and the extremity effects.

Figure 1 shows the layout of the experimental rig. The blade section model is jointed to a motorized strut that makes it oscillate in pitch about the 25% c axis. An encoder mounted directly on the model external shaft was used to get the instantaneous position of the model during the tests. The model pitching motion is controlled by means of an apposite code implementing a proportional and derivative control. More details about the pitching aerofoil experimental rig can be found in [20, 16].

2.1 Unsteady pressure measurement set up

The model central section is instrumented with 21 fast-response pressure transducers. The pressure taps are positioned around the model midspan airfoil contour as listed in Tab. 1.

Tap Number	1	2	3
Location x/c	0	0.01	0.044
Tap Number	4	5	6
Location x/c	0.096	0.164	0.28
Tap Number	7	8	9
Location x/c	0.358	0.453	0.618
Tap Number	10	11	12
Location x/c	0.76	0.9	0.9
Tap Number	13	14	15
Location x/c	0.767	0.628	0.459
Tap Number	16	17	18
Location x/c	0.373	0.285	0.185
Tap Number	19	20	21
Location x/c	0.118	0.06	0.02

Table 1: Pressure taps location on the NACA 23012 model midspan contour.

The lift and pitching moment during a pitching cycle were evaluated integrating the phase averaged pressures measured on the midspan contour of the model. The phase average of the pressure measurements was calculated using a bin of 0.1 deg. angle of attack amplitude. A National Instrument compact data acquisition system equipped with six 24 bit A/D simultaneous bridge modules with 4 channels each was employed to get the pressure measurements over 30 complete pitching cycles with a sampling rate of 50 kHz.

2.2 PIV set up

A double shutter CCD camera with a 12 bit, 1952×1112 pixel array and a 55 mm lens were used to acquire the image pairs. The measurement window covers the region around the L-shaped tab at the airfoil trailing edge to investigate the detailed flow physics around the L-shaped tab. A Nd:Yag double pulsed laser with 200 mJ output energy and a wavelength of 532 nm was used in the PIV system. The laser sheet passed through an opening in the wind tunnel roof aligned with the flow and positioned in the midspan of the test section width. The laser and the camera were mounted on a external metallic structure made of aluminium profiles that was connected to the heavy basement in order to avoid the transfer of the wind tunnel vibrations to the PIV measurement devices during the tests. A particle generator with Laskin nozzles was used for the flow insemination. The tracer particles, consisting in small oil droplets with a diameter within the range of 1-2 μm, were injected in correspondence of a section just after the fans and fulfill the wind tunnel volume with homogeneous density. The image pairs post-processing was carried out using the PIVview 2C software [21] of PIVTEC. Multigrid technique [22] was employed to correlate the image pairs, up to an interrogation window of 16×16 pixels. The velocity flow fields were phase averaged over 100 image pairs.

2.3 L-shaped tab

The L-shaped tab was manufactured using two carbon fiber skins. The tab has a 25 mm chord, is 0.5 mm thick and spans the entire blade sec-

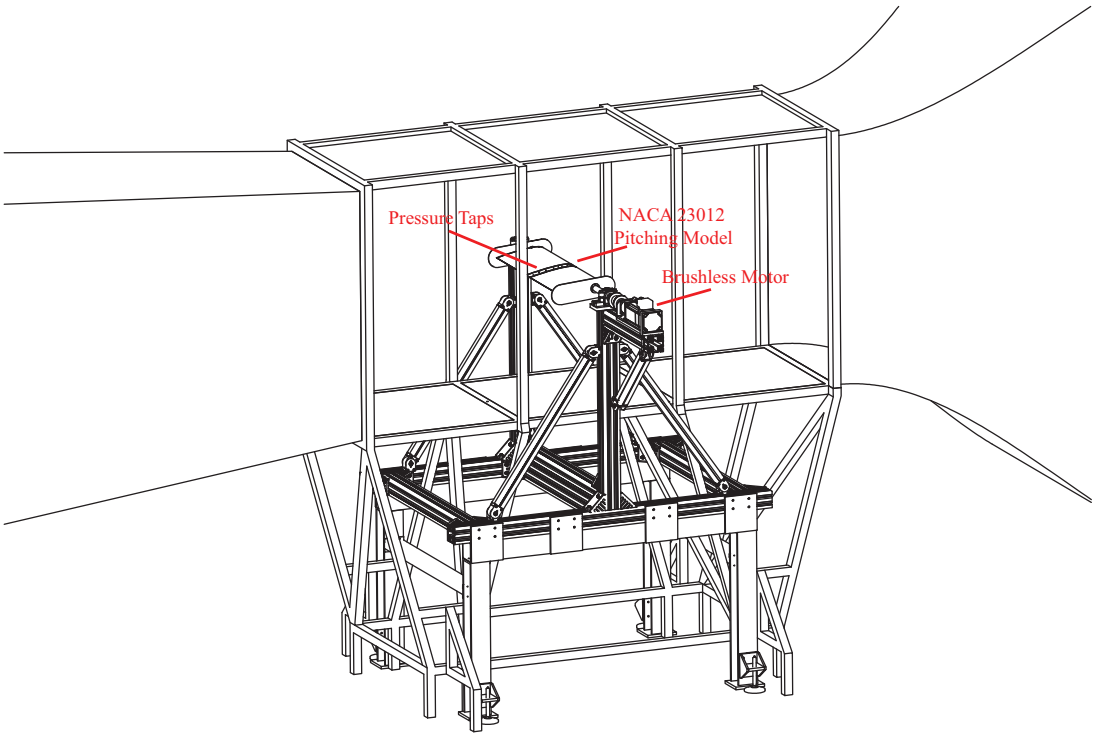

Figure 1: Layout of the experimental rig for pitching airfoils tests.

tion model. The L-shaped tab was attached on the model upper surface at the trailing edge region and was tested in two fixed positions illustrated in Fig. 2.

The L-shaped tab when deployed is flush with the airfoil upper surface so that the end prong behaves as a Gurney flap in correspondence of the trailing edge (see Fig. 2a). In this configuration the end prong of the tab protrudes 4 mm from the trailing edge corresponding to 1.3% c.

The L-shaped tab when retracted features an angle 9.1 deg. with the airfoil upper surface, since the prong tip touches the trailing edge (see Fig. 2b).

Figure 3 shows the blade section model equipped with the deployed L-shaped tab inside the wind tunnel test section.

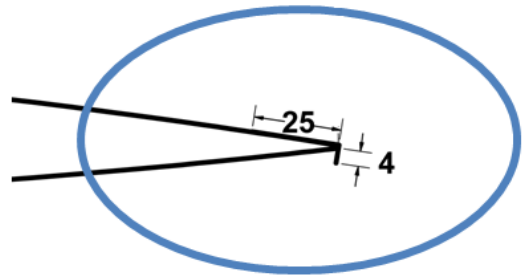

(a) L-tab deployed

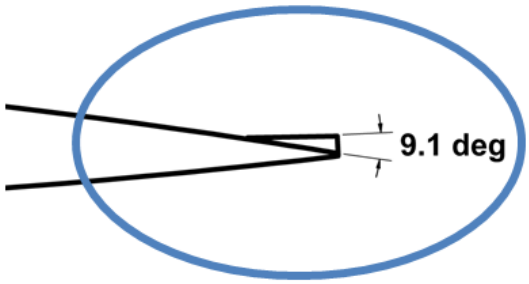

(b) L-tab retracted

Figure 2: Particular of the L-shaped tab layout at the NACA 23012 airfoil trailing edge (dimensions in mm).

3 Results and Discussion

The pitching cycle considered to evaluate the effects of the L-shaped is characterized by a mean angle of attack of $\alpha_m = 10°$, with oscillation amplitude of $\alpha_a = 10°$ and reduced frequency $k = 0.1$. This test condition corresponds to the deep dynamic stall regime ac-

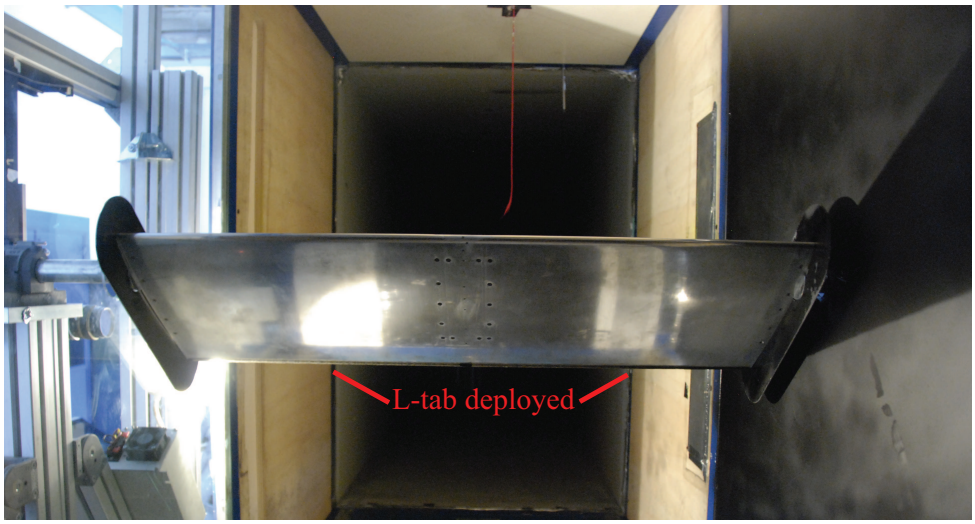

Figure 3: NACA 23012 blade section model inside the wind tunnel test section (L-shaped tab deployed).

cording to the definition of McCroskey [1], in which a portion of the upstroke is extended beyond the static stall angle. The tests were carried out at $U_\infty = 30$ m/s, corresponding to Re $= 6 \times 10^5$ and Ma $= 0.09$.

The phase averaged lift and quarter chord moment coefficients evaluated with the L-shaped tab deployed and retracted are illustrated in Fig. 4 compared to the airloads evaluated for the clean airfoil configuration. The standard deviation of the airloads coefficients are plotted on the curves.

The test results show that the deployed L-shaped tab, behaving as a Gurney flap, produces significant effects on the airloads. In fact, the lift and pitching moment curves are shifted in comparison to the clean airfoil configuration, in agreement with the results obtained by Chandrasekhara et al. [14] for a pitching VR-12 airfoil. On the other hand, the airloads evaluated for the retracted L-shaped tab configuration show smaller differences with respect to the clean configuration, (mostly in the part of the pitching cycle at low incidence) showing a behavior similar to a slightly upward deflected flap.

More details about the effects introduced by the L-shaped tab can be deduced from the comparison of the pressure coefficient distributions measured at $\alpha = 9°$ in upstroke (see Fig. 5). The lift increase observed with the L-shaped tab deployed is due to both a higher suction (lower pressure) on the upper surface and a higher pressure on the lower surface. These effects are spread over almost all the airfoil chord and are particularly relevant at the high velocity region. This lift increase introduced by a Gurney flap is often explained by the modification of the Kutta condition [14] due to the vortex structure past the Gurney flap itself, as it can be seen for example in the measured flow field shown in Fig. 7b. The local pressure increase at lower surface trailing edge is due the flow slowing down at the forward facing side of the Gurney flap. On the other hand, the C_p distribution measured with the the L-shaped tab retracted is very similar to the one measured for the clean airfoil. Therefore, the pressure data show that at this angle of attack the L-shaped tab retracted does not introduce the same remarkable effects upstream this device observed deploying the tab.

The overall behavior of the C_p measured on the airfoil upper surface during the upstroke motion is illustrated in Fig. 6. For the deployed L-shaped tab configuration, it can be observed a higher pressure peak spread over a larger angles of attack range with respect to the clean airfoil configuration. This feature is responsible of the production of a higher level of lift during upstroke and it is highlighted in Fig. 6 by the larger angle of attack range where the $-C_p$ contour levels are above 5 ($\Delta\alpha$ in Fig. 6a and b) . For the configuration with the L-

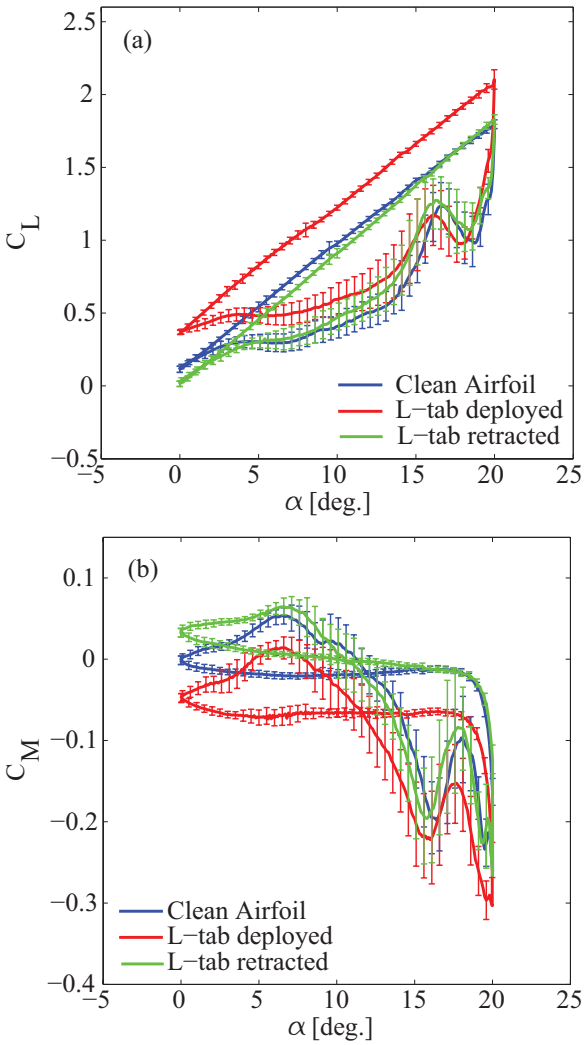

Figure 4: Comparison of the airloads curves measured with the L-shaped tab for $\alpha = 10° + 10° \sin(\omega t)$, $k = 0.1$ (Re $= 6 \times 10^5$ and Ma $= 0.09$).

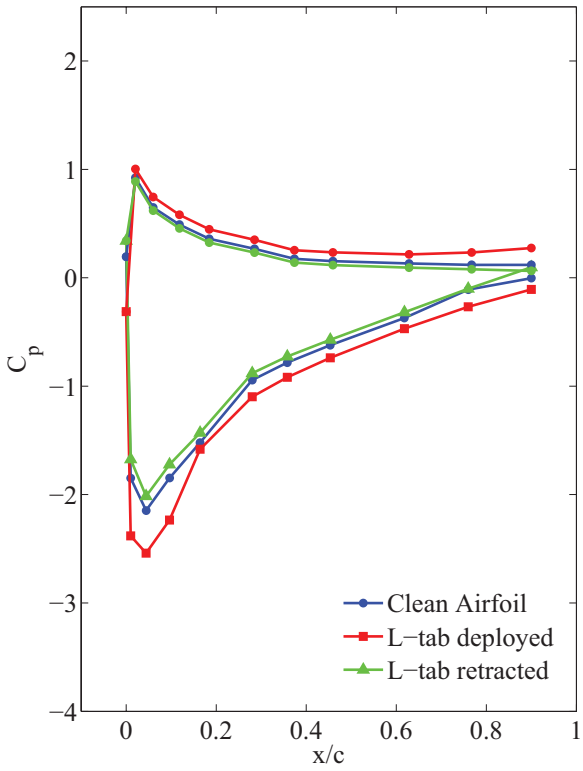

Figure 5: Comparison of the pressure coefficient distributions measured with the L-shaped tab at $\alpha = 9°$ upstroke.

shaped tab retracted the overall pressure time history in upstroke retraces quite the behavior of the clean airfoil configuration (see Fig. 6c).

The conspicuous lift coefficient increase observed during the upstroke motion when the L-shaped tab is deployed can be considered a benefit for the rotor performance due to an associated higher level of available thrust for the retreating blade. Moreover, the behavior of the pitching moment coefficient curves suggests that an active retraction of the L-shaped tab during the downstroke motion increases the C_M curve counterclockwise loop area associated to a positive aerodynamic damping and reduces the clockwise loop area associated to a negative aerodynamic damping [3]. Therefore, the test results show that the use of an active L-shaped tab deployed during the upstroke motion (to make it behaves as a Gurney flap) and retracted during downstrokethus would reduce the risk of stall flutter occurrence.

The discussion about the use of the L-shaped tab has to be completed with some considerations about the performance penalty introduced by drag increase. The present experimental activity do not give quantitative data about this issue as the total drag is not available from pressure measurements. Nevertheless, the drag measurement for a deep dynamic stall condition represents a very challenging activity due to the severe unsteadiness conditions typical of this phenomenon [23]. The attempt of to obtain the drag by means of wake phase averaged measurements did not succeed to produce a very accurate estimation as many sources of uncertainty are present in the problem.

The results of the numerical simulations by Yee et al. [11] carried outin steady conditions

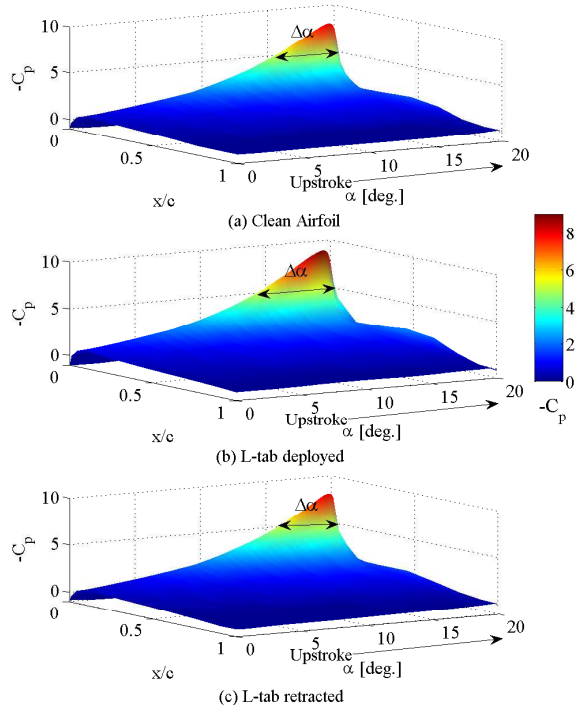

Figure 6: Comparison of the pressure coefficient time history on the NACA 23012 airfoil upper surface measured with the L-shaped tab in upstroke.

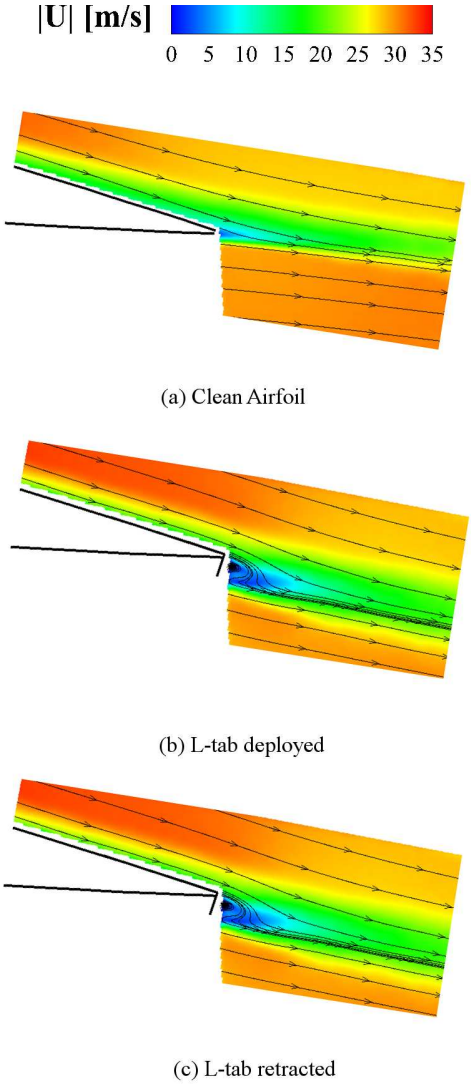

Figure 7: Comparison of the PIV flow fields measured at $\alpha = 9°$ in upstroke with the L-shaped tab.

on a NACA 0012 airfoil equipped with Gurney flaps with different height can give a possible estimation of the order of magnitude of the drag increase associated to the deployed L-shaped tab. According to this work, a maximum drag increase in the order of a few thousandth could be expected for the present deployed tab. On the contrary, even if no terms of comparisons were found, for the L-shaped tab in retracted configuration an effect of the same order in terms of drag penalty can be considered reasonable to be expected.

The flow field at the airfoil trailing edge region with and without the L-shaped tab was investigated by means of PIV surveys carried out at $\alpha = 9°$ in upstroke. Figure 7 show the PIV results by means of the velocity magnitude contours and the in-plane streamlines.

The flow at this angle of attack in upstroke is attached to the airfoil upper surface for the clean configuration, as it can be observed in Fig. 7a. The L-shaped tab deployed produces the downward deflection of the wake, while, as it occurs with a Gurney flap, behind the end prong of the tab a vortex structure with just one closed cell can be observed (see Fig. 7b). When the L-shaped tab is retracted the flow behind the end prong of the tab shows a structure that is essentially symmetrical with respect to the deployed tab case, in this case with the closed cell turning counterclockwise (see Fig. 7c).

4 Conclusions

An experimental activity was carried out on a pitching NACA 23012 airfoil in deep dynamic stall condition to evaluate the effects of a L-shaped tab positioned at the airfoil trailing edge for dynamic stall control purpose.

The pressure measurements show that benefits for the main rotor performance can be obtained with such an active controlled device. In particular, the tests results demonstrated that deploying the L-shaped tab during the upstroke motion (to make it behaves as a Gurney flap) and retracting the tab during downstroke can increase the retreating blade lift and reduce the risk of stall flutter occurrence. Moreover, PIV surveys were employed in the present activity results to evaluate the detailed flow physics related to the use of the L-shaped tab at the trailing edge region.

The main goal of the work was to investigate that advantages for dynamic stall alleviation similar to the ones that can be obtained with a deployable Gurney flap can be obtained with a device that show an easier installation on helicopter blades. In fact, the pivoting L-shaped tab could be easily integrated on the blade external surface, while its actuation mechanism could be stowed inside the blade upstream the trailing edge, where the space requirement are not particularly severe. Hence, the present experimental results encourage the research activity to manufacture and test this solution on a blade section model for dynamic stall control purpose.

Copyright Statement

References

[1] W.J. McCroskey. The Phenomenon of Dynamic Stall, NASA TM 81264, 1981.

[2] J.G. Leishman. Principles of helicopter aerodynamics, Cambridge University Press, 2006.

[3] F.O. Carta. An analysis of the stall flutter instability of helicopter rotor blades, *Journal of the American Helicopter Society*, **12**, 1Ű8, 1967.

[4] M. Chandrasekhara, P. Martin and C. Tung. Compressible dynamic stall control using a variable droop leading edge airfoil, *Journal of Aircraft*, **41**, 862Ű869, 2004.

[5] A. Gardner, K. Richter, H. Maiand D. Neuhaus. Experimental control of compressible oa209 dynamic stall by air jets, *38th European Rotorcraft Forum*, Amsterdam, The Netherlands, 4-7 September 2012.

[6] C. Singh, D. Peake, A. Kokkalis, V. Khodagolian, F. Coton and R. Galbraith. Control of rotorcraft retreating blade stall using air-jet vortex generators *Journal of Aircraft*, **43**, 1169Ű1176, 2006.

[7] M. Post and T. Corke. Separation control using plasma actuators: Dynamic stall vortex control on oscillating airfoil, *AIAA Journal*, **44**, 3125Ű3135, 2006.

[8] R.H. Liebeck. Design of subsonic airfoils for high lift, *Journal of Aircraft*, **15**, 547Ű561, 1978.

[9] J.A.C. Kentfield. The potential of gurney flaps for improving the aerodynamic performance of helicopter rotors, *AIAA International Powered Lift Conference*, AIAA Paper 93-4883, 1993.

[10] M.D. Maughmer and G. Bramesfeld. Experimental investigation of gurney flaps, *Journal of Aircraft*, **45**, 2062Ű2067, 2008.

[11] K. Yee, W. Joo and D.H. Lee. Aerodynamic performance analysis of a gurney flap for rotorcraft application, *Journal of Aircraft*, **44**, 1003Ű1014, 2007.

[12] H. Yeo. Assessment of active controls for rotor performance enhancement, *Journal of the American Helicopter Society*, **53**, 152Ű163, 2008.

[13] M.P. Kinzel and M.D. Maughmer. Numerical investigation on the aerodynamics of oscillating airfoils with deployable gurney flaps, *AIAA Journal*, **48**, 1457Ű1469, 2010.

[14] M. Chandrasekhara, P. Martin and C. Tung. Compressible dynamic stall performance of a variable droop leading edge airfoil with a gurney flap, *Journal of the American Helicopter Society*, **53**, 18Ű25, 2008.

[15] A. Zanotti and G. Gibertini. Experimental investigation of the dynamic stall phenomenon on a NACA 23012 oscillating airfoil, *Proceedings of the Institution of Mechanical Engineers, Part G: Journal of Aerospace Engineering*, Epub ahead of print 20 July 2012, doi:10.1177/0954410012454100.

[16] A. Zanotti, F. Auteri, G. Campanardi and G. Gibertini. An Experimental Set Up for the Study of the Retreating Blade Dynamic Stall, *37th European Rotorcraft Forum*, Gallarate (VA), Italy, 13-15 September 2011.

[17] J.G. Leishman. Dynamic stall experiments on the NACA 23012 airfoil, *Experiments in Fluids*, **9**, 49-58, 1990.

[18] A. Zanotti, S. Melone, R. Nilifard and A. D'Andrea. Experimental-numerical investigation of a pitching airfoil in deep dynamic stall, *Proceedings of the Institution of Mechanical Engineers, Part G: Journal of Aerospace Engineering*, Epub ahead of print 26 February 2013, doi:10.1177/0954410013475954.

[19] A. Zanotti, G. Gibertini, D. Grassi and D. Spreafico. Wake Measurements behind an Oscillating Airfoil in Dynamic Stall Conditions, *ISRN Aerospace Engineering*, **2013**, 1-11, 2013.

[20] A. Zanotti. Retreating Blade Dynamic Stall, Ph.D. thesis, Politecnico di Milano, 2012.

[21] PIVview 2C version 3.2, User Manual, PIVTEC, www.pivtec.com.

[22] Raffel M, Willert C and Kompenhans J. *Particle Image Velocimetry, a practical guide*. Springer, Heidelberg, 1998.

[23] G. Gibertini, F. Auteri, D. Grassi, D. Spreafico and A. Zanotti. Experimental method for drag measurement of an oscillating airfoil in dynamic stall condition, *38th European Rotorcraft Forum*, Amsterdam, The Netherlands, 4-7 September 2012.